

## NOTE

Efficient Computation of Spatial Eigenvalues  
for Hydrodynamic Stability Analysis

## 1. INTRODUCTION

The present paper outlines a simple procedure for spatial stability computations which substantially reduces the computational cost of performing such analyses. Using several different external and internal flow examples, the usefulness of the procedure is clearly demonstrated.

The final form for linear stability analyses (whether temporal or spatial) can be represented as a generalized eigenvalue problem,

$$AX = \lambda BX, \quad (1)$$

regardless of the numerical method employed to discretize the governing ordinary differential equations. In Eq. (1)  $A$  and  $B$  are the discretized coefficient matrices,  $X$  is the eigenfunction vector, and  $\lambda$  is the eigenvalue which represents the complex disturbance frequency for temporal stability and disturbance wave number for spatial stability problems. Global analysis, as opposed to local analysis, is needed for solving such systems since it does not require any initial guess and the entire eigenvalue spectrum can be obtained by using methods such as QZ [1]. Although the global calculation has become routine in temporal analyses, its application to spatial stability analyses is comparatively very expensive. The high computational cost is due to the fact that in spatial analysis, the eigenvalue appears nonlinearly in the governing equations. Applying a simple transformation (cf. Bridges and Morris [2], Bramley [3], Khorrami *et al.* [4]), the quadratic terms for the eigenvalue are linearized. Such a transformation results in matrices  $A$  and  $B$  which are almost twice as large as those for the temporal case. Since the computational cost for the global solution using the QZ algorithm is of  $O(m^3)$ , where  $m$  is the order of coefficient matrices, the spatial analysis is about five to six times more expensive than a temporal stability analysis. Obviously, any reduction in the order of  $A$  and  $B$  results in substantial savings in computational resources (both memory size and computational time). Such savings would be valuable for spatial secondary stability analysis where the order of  $A$  or  $B$  is already two to three times larger even in temporal analyses.

One approach to reduce the computational cost was recently suggested by Malik [5]. This approach stems from the realization that the nonlinearity in the spatial eigenvalue is caused by the streamwise diffusion terms ( $\partial^2 u / \partial x^2$ ,  $\partial^2 T / \partial x^2$ , etc.) which, in most shear flows, is much less significant than the cross-stream diffusion. For inviscid instability where viscosity acts only to stabilize the flow, the insignificance of the streamwise diffusion terms is very apparent. However, neglecting this term for viscous instability needs some justification.

For wall-bounded flows, viscosity becomes singularly important in a thin layer near the wall. However, an asymptotic analysis indicates that only the wall-normal diffusion terms significantly contribute to the viscous instability. In fact, Smith *et al.* [6] show that the viscous instability problem for a boundary layer at finite-Reynolds numbers can be formulated by using interacting boundary layer equations which ignore streamwise diffusion terms. The basic idea here is that the neglect of streamwise diffusion would not alter the fundamental structure of the instability (viscous or inviscid) and the dominant physics will be captured, although the disturbance growth rate may be in error. If the streamwise diffusion terms ( $\partial^2 / \partial x^2$ , etc.) and thus the quadratic terms in wave number are dropped, the order of matrices  $A$  and  $B$  reduces to that of the temporal stability arrangement. As a result, the important (desired) half of the spatial eigenvalue spectrum can be computed with the same computational resources as the temporal spectrum. The approximate eigenvalues can then be corrected using local calculations which can be performed for temporal and spatial problems with equal efficiency. However, it must be emphasized here that such a major reduction in the order of  $A$  and  $B$  is possible only when the primitive form of the governing equations is considered. This is generally the case. For those problems which can be represented by the Orr-Sommerfeld equation, no such gain is possible. In these situations, even though dropping the streamwise diffusion term results in a modest reduction in the size of the coefficient matrices, spatial stability calculations will always be more expensive than temporal calculations.

In the following sections, the viability of the above procedure is demonstrated for the cases of plane Poiseuille flow, the trailing line vortex, and the Blasius boundary layer (incompressible and compressible). The instability in the Poiseuille flow is viscous while the trailing line vortex has both viscous and inviscid instability modes. Similarly, a compressible boundary layer is subjected to viscous instability at low Mach numbers while the dominant instability is inviscid in nature for high Mach numbers. Thus, the examples cover a wide range of flows and illustrate the usefulness of the approach described above.

### 2. ANALYSIS

The governing differential equations for hydrodynamic stability analysis are of the form

$$(\alpha^2 L_0 + \alpha L_1 + L_2)\phi = 0, \tag{2}$$

where  $L_i$  ( $i = 0, 1, 2$ ) are linear differential operators,  $\alpha$  is the spatial eigenvalue, and  $\phi$  the corresponding eigenfunction. The differential equation (2) can be discretized by using finite-difference or spectral approach to yield

$$(E_2 + \alpha E_1 + \alpha^2 E_0)\bar{\phi} = 0, \tag{3}$$

where  $E_0$ ,  $E_1$ , and  $E_2$  are  $N \times N$  matrices and  $N$  is the number of grid points. The discrete problem (3) can be solved, for example, by the companion matrix approach (Ref. [2]) yielding  $2N$  eigenvalues. However, if coefficients of  $\alpha^2$  are small then (3) can be reduced to

$$(E_2 + E_1 \alpha)\bar{\phi} = 0 \tag{4}$$

which has only  $N$  eigenvalues. Thus, half the spatial eigenvalue spectrum is lost by the above approximation. However, the  $N$  eigenvalues of (4) contain the important eigenvalues for the hydrodynamic stability problem. In order to see which members of the spectrum of (3) are lost by the above approximation, we consider the scalar quadratic equation

$$\epsilon x^2 - 2bx + c = 0 \tag{5}$$

with  $b, c$  real numbers and  $\epsilon$  small. The roots of (5) are

$$x = \frac{b}{\epsilon} \pm \frac{b}{\epsilon} \sqrt{1 - \epsilon(c/b^2)} = \begin{cases} \frac{2b}{\epsilon} - \frac{c}{2b} + O(\epsilon) \\ \frac{c}{2b} + O(\epsilon). \end{cases}$$

Therefore, as  $\epsilon \rightarrow 0$  one of the roots of (5) approaches a root of the linearized version  $-2bx + c = 0$  and the other root

goes off to infinity. This is also what happens in the hydrodynamic stability problem since the eigenvalues of small modules are important in this case. Obviously, the above approximation will work only for certain types of physical problems.

We note that  $\alpha^2$  term appears in the momentum and energy equations but not in the continuity equation. Thus, for three-dimensional compressible boundary layers (3 momentum equations, 1 energy equation, and 1 continuity equation) the proposed approximation will yield a spectrum of  $5N$  eigenvalues instead of a full spectrum of  $9N$  eigenvalues.

### 3. PLANE POISEUILLE FLOW

The mean velocity profile for this flow is prescribed by

$$\begin{aligned} U &= 1 - y^2 \\ V &= 0, \end{aligned} \tag{6}$$

where  $U$  and  $V$  are the streamwise and normal velocities, respectively. Superposed on this flow are two-dimensional perturbations of the form

$$\{u, v, p\} = \{F(y), G(y), P(y)\} e^{i(\alpha x - \omega t)}, \tag{7}$$

where  $\alpha$  is the wave number and  $\omega$  the frequency. The linearized governing equations, in Cartesian coordinates ( $x, y, z$ ), for incompressible viscous flow in a channel are

Continuity,

$$i\alpha F + \frac{dG}{dy} = 0; \tag{8}$$

x-momentum,

$$\frac{d^2 F}{dy^2} + i\omega \text{Re } F - i\alpha \text{Re } UF - \alpha^2 F - \text{Re } \frac{dU}{dy} G - i\alpha \text{Re } P = 0, \tag{9}$$

y-momentum,

$$\frac{d^2 G}{dy^2} + i\omega \text{Re } G - i\alpha \text{Re } UG - \alpha^2 G - \text{Re } \frac{dP}{dy} = 0, \tag{10}$$

where  $u$  and  $v$  are the velocity perturbations and  $F$  and  $G$  are the corresponding eigenfunctions in the  $x$ - and  $y$ -directions, respectively, and  $p$  is the pressure perturbation.  $\text{Re}$  is the Reynolds number based on half width,  $h$ , and centerline velocity of the channel. The boundary conditions are

$$F(\pm 1) = G(\pm 1) = 0. \tag{11}$$

These equations are discretized using a Chebyshev spectral collocation technique with a staggered grid. Staggering the pressure terms along with the continuity equation eliminates the need for any pressure boundary conditions. The mathematical details of the spectral method can be found in Gottlieb *et al.* [7] and Canuto *et al.* [8] and are omitted here. Implementation of the staggered grid is described by Khorrami [9] and by Macaraeg *et al.* [10].

If the  $\alpha^2$  terms are dropped from Eqs. (8)–(10), the generalized eigenvalue problem becomes

$$A\mathbf{X} = \alpha B\mathbf{X},$$

where

$$\mathbf{X} = [F G P]^T. \quad (12)$$

For this problem,  $A$  and  $B$  are of  $O(3N)$ , where  $N$  is the number of collocation points. However, if the  $\alpha^2$  terms are retained, then the transformation

$$\begin{aligned} \bar{F} &= \alpha F \\ \bar{G} &= \alpha G \end{aligned} \quad (13)$$

is needed to linearize the quadratic terms. The extra boundary conditions are

$$\bar{F}(\pm 1) = \bar{G}(\pm 1) = 0. \quad (14)$$

In this format, the eigenvector becomes

$$\mathbf{X} = [F G P \bar{F} \bar{G}]^T. \quad (15)$$

The coefficient matrices now turn out to be  $O(5N)$ , which is substantially larger than those in Eq. (12). Throughout this study, the complex IMSL QZ routine is employed to obtain the eigenvalue spectrum. The cost of computing the eigenvalue spectrum from Eq. (12) using this algorithm is only about 20% of that required for Eq. (15).

TABLE I

Spatial Eigenvalue  $\alpha$  for Plane Poiseuille Flow Using  $\omega = 0.26$ ,  $Re = 6000$

$N$	a	$N$	b
35	1.000472 - i0.000866	36	1.0004686 - i0.0013015
36	1.000478 - i0.000862	40	1.0004657 - i0.0013004
37	1.000473 - i0.000856	44	1.0004654 - i0.0013004
38	1.000472 - i0.000863	48	1.0004654 - i0.0013005
39	1.000472 - i0.000859	50	1.0004654 - i0.0013004
40	1.000473 - i0.000859		
41	1.000471 - i0.000860		
42	1.000465 - i0.000863		

Note. a.  $\alpha^2$  terms included; b.  $\alpha^2$  terms dropped.

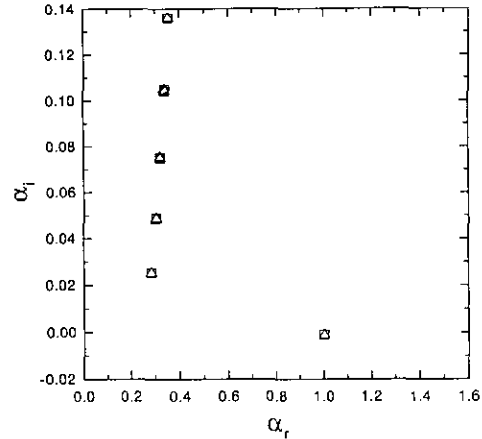


FIG. 1. The first 10 eigenvalues for plane Poiseuille flow:  $\square$  with  $\alpha^2$ ;  $\triangle$  without  $\alpha^2$  terms;  $\omega = 0.26$ ,  $Re = 6000$ , and  $N = 40$ .

Spatial eigenvalue  $\alpha$  was computed for  $\omega = 0.26$  and  $Re = 6000$  and the results are presented in Table I for various numbers of Chebyshev polynomials. We note that the instability at this frequency is viscous in nature. The resulting eigenvalue with the  $\alpha^2$  terms included is in excellent agreement (not shown) with the eigenmode obtained by Bridges and Morris [2]. Note the presence of a slight round off error as  $N$  is increased beyond 40. Table I also shows results with the quadratic terms in  $\alpha$  dropped. The imaginary part indicates that such exclusion results in a stronger instability while the real part of  $\alpha$  is hardly changed. In this case, roundoff error is less apparent due to the smaller size of the  $A$  and  $B$  matrices. The initial guess for  $\alpha$  ( $1.000465690 - i0.001300430$ ) from Table I with  $N = 40$  was used in a local method, with the full equations, and the eigenvalue in Column I was recovered. The first 10 eigenvalues of the spatial spectrum associated with both neglecting and retaining the  $\alpha^2$  terms are potted in Fig. 1. This figure confirms that omitting the nonlinear terms in  $\alpha$  does not effect the spectrum significantly.

#### 4. TRAILING LINE VORTEX

In cylindrical-polar coordinates  $(r, \theta, x)$ , following Lessen *et al.* [11], the mean velocity profile for the trailing line vortex is given by

$$\begin{aligned} U &= 0 \\ V &= \frac{q}{r} (1 - e^{-r^2}) \\ W &= 1 + e^{-r^2}, \end{aligned} \quad (16)$$

where  $U$ ,  $V$ , and  $W$  are the non-dimensional radial, azimuthal, axial velocities, respectively, and  $q$ , the swirl parameter, is proportional to the ratio of maximum swirl

TABLE II

Eigenvalues  $\alpha$  for the First Two Inviscid Unstable Modes in Trailing Line Vortex

$N$	a	b
40	1.3082708 - $i$ 0.1831288	1.3082463 - $i$ 0.1832364
	1.3419196 - $i$ 0.1026364	1.3419181 - $i$ 0.1027435
44	1.3082708 - $i$ 0.1831287	1.3082463 - $i$ 0.1832364
	1.3419461 - $i$ 0.1026388	1.3419445 - $i$ 0.1027460
48	1.3082709 - $i$ 0.1831288	1.3082463 - $i$ 0.1832364
	1.3419367 - $i$ 0.1026344	1.3419349 - $i$ 0.1027416
52	1.3082709 - $i$ 0.1831288	1.3082463 - $i$ 0.1832364
	1.3419355 - $i$ 0.1026353	1.3419341 - $i$ 0.1027422

Note. a.  $\alpha^2$  terms included; b.  $\alpha^2$  terms dropped ( $\omega = 1.0$ ,  $n = -2$ ,  $q = 0.8$ ,  $Re = 10,000$ ).

velocity to maximum axial velocity as given in Lessen *et al.* [11]. Assuming three-dimensional perturbations of the form

$$\{u, v, w, p\} = \{iF(r), G(r), H(r), P(r)\} e^{i(\alpha x + n\theta - \omega t)}, \quad (17)$$

the linearized governing equations are given by Lessen *et al.* [11] and by Khorrami *et al.* [4]. In Eq. (17),  $n$  is the azimuthal wave number which can only take on integer values.

Again we choose Chebyshev spectral collocation for conducting the computations (Khorrami *et al.* [4]). The size of coefficient matrices is  $O(4N)$  or  $O(7N)$ , depending on whether  $\alpha^2$  terms are dropped or retained.

Using both the full and reduced (linearized) set of equations, the first two inviscidly unstable modes for a representative set of parameters  $\omega = 1.0$ ,  $n = -2$ ,  $q = 0.8$ , and  $Re = 10,000$  are shown in Table II. The agreement between

TABLE III

Eigenvalue  $\alpha$  for the Axisymmetric Viscous Mode in Trailing Line Vortex

$N$	a	b
40	0.51682118 - $i$ 0.00018681	0.51682118 - $i$ 0.00021430
44	0.51682123 - $i$ 0.00018689	0.51682120 - $i$ 0.00021430
48	0.51682126 - $i$ 0.00018692	0.51682124 - $i$ 0.00021426
52	0.51682116 - $i$ 0.00018687	0.51682124 - $i$ 0.00021426

Note. a.  $\alpha^2$  terms included; b.  $\alpha^2$  terms dropped ( $\omega = 0.5$ ,  $n = 0$ ,  $q = 1.0$ ,  $Re = 10,000$ ).

the two sets of results is excellent. Overall, the variations are of the order  $1/Re$  which may be neglected due to the large growth rates of inviscid disturbances. In fact in this case there is no need to refine the computed eigenvalues using a local scheme. Figure 2 is the plot of the first 10 eigenvalues from the spectra associated with Table II. The agreement between the two data sets confirms that the eigenvalue spectrum for the inviscid modes is virtually insensitive to the exclusion of nonlinear terms. One might argue that there is no need for solving the viscous equations for this problem since the inviscid instability is described by Rayleigh's equation. However, it is well known (in the case of a trailing line vortex, see Leibovich and Stewardson [12]) that there is a severe case of a non-convergent solution and mode jumping near the neutral points when the inviscid equations alone are considered. Thus, the viscous terms are needed to extend the computation beyond the upper and lower neutral curves.

The axisymmetric ( $n = 0$ ) viscous mode of instability for the trailing-line vortex is shown in Table III, with and without  $\alpha^2$  terms. As expected, the increase in the growth rate is of order  $1/Re$ . For the  $n = 0$  mode, the shift in the imaginary part of the wavenumber is not as large as in the

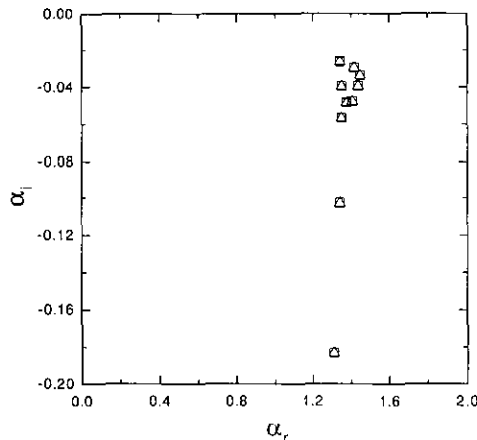


FIG. 2. The first 10 inviscid modes of a trailing line vortex:  $\square$  with  $\alpha^2$ ,  $\triangle$  without  $\alpha^2$  terms;  $\omega = 1.0$ ,  $n = -2$ ,  $q = 0.8$ ,  $Re = 10,000$ , and  $N = 52$ .

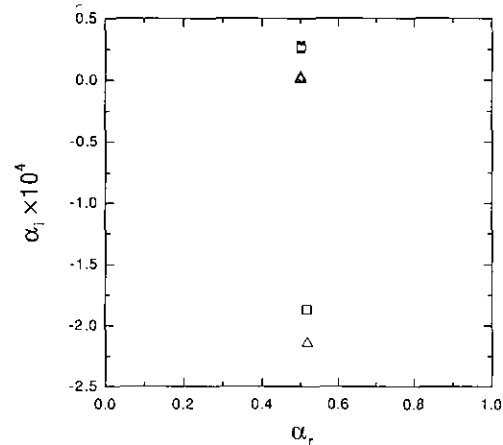


FIG. 3. The first 10 viscous modes of a trailing line vortex:  $\square$  with  $\alpha^2$ ,  $\triangle$  without  $\alpha^2$  terms;  $\omega = 0.5$ ,  $n = 0$ ,  $q = 1.0$ ,  $Re = 10,000$ , and  $N = 48$ .

TABLE IV

Spatial Eigenvalue  $\alpha$  for the Asymmetric Viscous Mode in Trailing Line Vortex

$N$	a	b
40	0.27981693 - $i$ 0.00033767	0.27981651 - $i$ 0.00037174
44	0.27981656 - $i$ 0.00033799	0.27981647 - $i$ 0.00037172
48	0.27981689 - $i$ 0.00033897	0.27981651 - $i$ 0.00037176
52	0.27981676 - $i$ 0.00033752	

Note. a.  $\alpha^2$  terms included; b.  $\alpha^2$  terms dropped ( $\omega = 0.3, n = 1, q = 0.4, Re = 2000$ ).

case of plane Poiseuille flow. The first 10 eigenvalues of the respective spectra are plotted in Fig. 3. Note that, except for the unstable mode, the eigenvalues are closely packed and difficult to distinguish. It is clear that omission of the  $\alpha^2$  terms shifts the stable modes toward the neutral curve, but they never cross it. Results for the asymmetric ( $n = 1$ ) viscous mode are presented in Table IV. The trends for this mode are identical to those explained for the axisymmetric disturbance.

As for the CPU time, obviously it is very much dependent on the type of computer utilized. However, independent of the test case, the amount of CPU time spent by the QZ routine to obtain the full eigenvalue spectrum is consistently at least three to four times greater than the amount spent for the reduced formulation. For example, for the case of  $\omega = 1.0, n = -2, q = 0.8, Re = 10,000$ , and  $N = 60$ , the respective CPU times on the NASA Langley's CRAY Y-MP are 9.2 and 2.3 s.

5. COMPRESSIBLE BLASIUS BOUNDARY LAYER

The governing equations for the basic state of the compressible Blasius boundary layer can be derived using the Levy-Lees transformation:

$$d\zeta \equiv \rho_e \mu_e u_e dx \tag{18}$$

$$d\eta \equiv [\rho_e u_e / (2\zeta)^{1/2}] (\rho / \rho_e) dy, \tag{19}$$

where  $\rho_e$  is the edge density,  $\mu_e$  is the edge viscosity,  $u_e$  is the streamwise edge velocity,  $x$  is the distance along the body, and  $y$  is normal to the body. In  $\zeta - \eta$  coordinates, the governing equations for the boundary layer with zero pressure gradient may be written as

$$(cf'')' + ff' = 0 \tag{20}$$

$$(a_1 g' + a_2 f'f'')' + fg' = 0, \tag{21}$$

where

$$f' \equiv u/u_e, \quad c \equiv \rho\mu/\rho_e\mu_e,$$

$$g \equiv H/H_e, \quad a_1 \equiv c/\sigma,$$

$$a_2 \equiv \frac{(\gamma - 1) M^2}{1 + ((\gamma - 1)/2) M^2} \left(1 - \frac{1}{\sigma}\right) c.$$

$H$  is the enthalpy,  $\gamma$  the ratio of specific heats, and  $M$  the edge Mach number defined as

$$M = u_e / \sqrt{\gamma \mathfrak{R} T_e}. \tag{22}$$

The Prandtl number  $\sigma$  is defined as

$$\sigma = \mu c_p / k, \tag{23}$$

where  $c_p$  is the specific heat at constant pressure and is assumed to be constant. The viscosity  $\mu$  is assumed to be given by the Sutherland formula,

$$\mu = 2.27 \times 10^{-8} \frac{T^{1/2}}{1 + 198.6/T} \text{ lb} - \text{s/ft}^2,$$

where  $T$  = static temperature in degrees °R.

The thermal conductivity  $k$  may be prescribed by a similar formula, but for the results presented in this paper we assume  $\sigma = 0.7$ .

We make a quasi-parallel flow approximation and impose velocity, pressure, and temperature perturbations of the form

$$\{\tilde{u}, \tilde{v}, \tilde{w}\} = \{\tilde{u}(y), \tilde{v}(y), \tilde{w}(y)\} e^{i(\alpha x + \beta z - \omega t)} \tag{24}$$

$$\tilde{p} = \tilde{p}(y) e^{i(\alpha x + \beta z - \omega t)} \tag{25}$$

$$\tilde{T} = \tilde{T}(y) e^{i(\alpha x + \beta z - \omega t)}, \tag{26}$$

where  $\alpha, \beta$  are the wavenumbers and  $\omega$  is the frequency.

It can be shown that linear disturbances satisfy the system of ordinary differential equations

$$(L_1 D^2 + L_2 D + L_3)\phi = 0, \tag{27}$$

TABLE V

Description of Test Cases

Test case	Mach number	$R$	$T_w/T_{amb}$	$T_0^0 R$	$\delta^*$
1	$10^{-6}$	580	1	500	1.7208
2	0.5	2000	1	500	1.8236
3	2.5	3000	1	600	4.2578

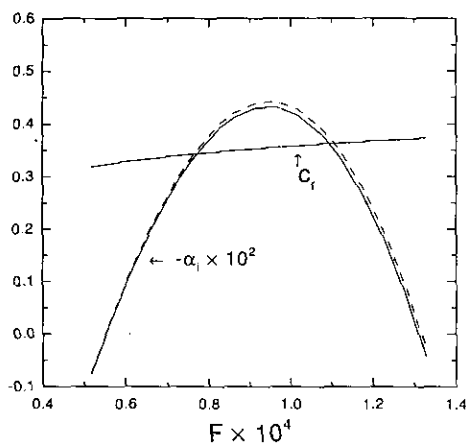


FIG. 4. Variation of the spatial growth rate and phase velocity vs frequency, — with  $\alpha^2$  terms, ----  $\alpha^2$  terms missing;  $M = 10^{-6}$ .

where  $\phi$  is a five-element vector defined by

$$[\hat{u}, \hat{v}, \hat{p}, \hat{T}, \hat{w}]^T.$$

Here  $D \equiv d/dy$ , while  $L_1$  is a diagonal matrix and  $L_2$  and  $L_3$  are  $5 \times 5$  matrices whose elements are given in [5].

We solve the above system of equations, with and without  $\alpha^2$  terms, using the method discussed by Malik [5]. With  $\alpha^2$  terms included, the order of  $A$  and  $B$  in (1) is  $9N$  while it drops to  $5N$  when  $\alpha^2$  terms are neglected.

Results have been obtained for three different Mach numbers as listed in Table V. The growth rate ( $-\alpha_i$ ) and phase velocity ( $c_r$ ) of the least stable mode for Case 1 are plotted in Fig. 4. It can be seen that there is very little consequence of neglecting the streamwise diffusion terms. The agreement between the two approaches (not shown) was even better for Mach 0.5 and 2.5 flows.

In three-dimensional boundary layers, the difference between the two approaches would depend upon the coordinate system and if it is chosen such that one of the axis aligns locally with the inviscid streamline then the difference between the two eigenvalues will be small.

## CONCLUSIONS

A simple method is presented in which the important half of the spatial global eigenvalue spectrum can be obtained

with the same computational effort as for the temporal problem. The method is demonstrated for a number of test problems including incompressible and compressible flows as well as viscous and inviscid instability modes. Since streamwise diffusion contributes little to the stability problem, excellent estimates of the spatial eigenvalues may be obtained by the proposed method.

## ACKNOWLEDGMENTS

The authors thank the reviewers for their excellent comments particularly the referee who suggested the example given in Eq. (5). This work was supported by NASA Langley Research Center under Contract NAS1-18240.

## REFERENCES

1. G. H. Golub and C. F. Van Loan, *Matrix Computations*, 2nd ed. (The Johns Hopkins University Press, Baltimore, MD, 1989).
2. T. J. Bridges and P. J. Morris, *J. Comput. Phys.* **55**, 437 (1984).
3. J. S. Bramley, *J. Comput. Phys.* **53**, 524 (1984).
4. M. R. Khorrami, M. R. Malik, and R. L. Ash, *J. Comput. Phys.* **81**, 206 (1989).
5. M. R. Malik, *J. Comput. Phys.* **86**, 376 (1990).
6. F. T. Smith, D. Papageorgiou, and J. W. Elliott, *J. Fluid Mech.* **146**, 313 (1984).
7. D. Gottlieb, M. Y. Hussaini, and S. A. Orszag, "Theory and Application of Spectral Methods," in *Spectral Methods for Partial Differential Equations*, edited by R. G. Voight, D. Gottlieb, and M. Y. Hussaini (Soc. Indus. & Appl. Math., Philadelphia, 1984), p. 1.
8. C. Canuto, M. Y. Hussaini, A. Quarteroni, and T. A. Zang, *Spectral Methods in Fluid Dynamics* (Springer-Verlag, New York, 1988).
9. M. R. Khorrami, *Int. J. Numer. Methods Fluids* **12**, 825 (1991).
10. M. G. Macaraeg, C. L. Streett, and M. Y. Hussaini, NASA TP 2858, 1988 (unpublished).
11. M. Lessen, P. J. Singh, and F. Paillet, *J. Fluid Mech.* **63**, 753 (1974).
12. S. Leibovich and K. Stewartson, *J. Fluid Mech.* **126**, 335 (1983).

Received February 15, 1991; accepted February 8, 1992

MEHDI R. KHORRAMI  
MUJEEB R. MALIK

High Technology Corporation  
P.O. Box 7262  
Hampton, Virginia 23666